Crystal-field levels and magnetic susceptibility in PuO_2

M. Colarieti-Tosti,[1,2] O. Eriksson,[1] L. Nordström,[1] J. Wills,[3] and M. S. S. Brooks[1,2]
[1]*Condensed Matter Theory Group, Uppsala University, Box 530, S-751 21 Uppsala, Sweden*
[2]*European Commission, Joint Research Centre, Institute for Transuranium Elements, Postfach 2340, D-76125 Karlsruhe, Germany*
[3]*Center for Materials Science and Theoretical Division, Los Alamos National Laboratory, Los Alamos, New Mexico 87545*
(Received 18 July 2001; revised manuscript received 9 October 2001; published 18 April 2002)

Ground-state electronic structure and crystal-field levels of PuO_2 have been calculated by means of a *symmetry constrained* local density approximation to density-functional theory in terms of total energy differences. The calculated Γ_1 (ground state) to Γ_4 (first excited state) excitation energy of 99 meV is in reasonable agreement with the measured value 123 meV from inelastic-neutron-scattering experiments. The measured magnetic susceptibility has been analyzed and its discrepancy with neutron-scattering results is partially removed by the introduction of antiferromagnetic exchange enhancement.

DOI: 10.1103/PhysRevB.65.195102 PACS number(s): 71.70.Ch, 75.10.Dg

I. INTRODUCTION

The first approximation to the ground state of the $5f$ electrons in PuO_2 is a $5f^4$ configuration which, in the Russell-Saunders coupling scheme, has $J=4$ with a g factor of 3/5. In a cubic symmetry the ninefold $J=4$ multiplet should split into $\Gamma_1(1)$, $\Gamma_3(2)$, $\Gamma_4(3)$, and $\Gamma_5(3)$ crystal field levels (values in parenthesis denote level degeneracy). The observed temperature independent magnetic susceptibility[1] suggests that the ground state is the nonmagnetic $\Gamma_1(1)$ singlet. Interpretation[1] of the observed magnetic susceptibility in terms of a single transition from a nonmagnetic Γ_1 ground state yielded an excitation energy of 284 meV. Recent inelastic-neutron-scattering experiments[2] detected one excitation, evidently $\Gamma_1 \rightarrow \Gamma_4$ (if Γ_1 is the ground state) at 123 meV. The magnetic dipole transitions $\Gamma_3 \rightarrow \Gamma_4$ and $\Gamma_3 \rightarrow \Gamma_5$ are also allowed but would only be consistent with experiment if the nonmagnetic Γ_3 doublet were the ground state. However, the measured temperature independent magnetic susceptibility excludes this possibility. The difference by a factor of more than 2 for the $\Gamma_1 \rightarrow \Gamma_4$ excitation energy evaluated from two measurements[1,2] is an anomaly that it is desirable to address with theory.

It has recently become possible to make *ab initio* calculations of crystal-field energy levels and electric field gradients,[3–10] usually for rare-earth metals and compounds. The normal approach is based upon perturbation theory as in the standard model for crystal fields.[3–8] The f electron density is approximated by a spherical density as in a free atom calculation, frequently with the use of the self-interaction correction.[11,12] The remaining conduction electron density is obtained from the otherwise full-potential energy band calculations resulting in aspherical Coulomb and exchange potentials at the rare-earth sites. The crystal-field parameters are then calculated directly from integrals of products of the aspherical parts of the potentials and spherical f densities and there is a division into onsite and lattice contributions to the potential and crystal-field parameters. Results have been promising if not always very accurate and experience has shown that the calculated crystal-field parameters are sensitive to whether or not the self-interaction correction is used.

The method used here is not based upon perturbation theory. The total energy is computed for each crystal-field state for which the $5f$ density has its correct aspherical shape.[13] The conduction electron density is allowed to screen changes in $5f$ density when the crystal-field state is changed. The crystal-field excitation energies are the differences between these total energies. High relative accuracy is required but larger errors in the total energies are expected to cancel. Compared to previous works on rare earths,[13,14] the application to actinides is expected to be even more challenging since the $5f$ states are less well bound than $4f$ states and likely to be even more sensitive to approximations to the potential. The present work should therefore be viewed as exploratory. We do not expect to be able to calculate the crystal fields in actinide compounds to an accuracy of a meV but would hope to obtain the correct ground state and a good estimate of the order of magnitude of the energies of excited states. A positive factor is that the crystal-field splittings in actinide dioxides are very large (typically 100 meV) compared to those in rare-earth compounds (typically 10 meV) therefore it is not necessary to have an accuracy of one meV to obtain good agreement with experiments.

The rest of this paper is organized as follows. The method and calculated ground-state band structure is discussed in Sec. II. Details of the constraints applied to the localized $5f$ states are given in Sec. III as are the effects of different approximations for the $5f$ potential.[14] In Sec. IV we discuss the calculated results and magnetic susceptibility concluding that antiferromagnetic exchange is required to make the susceptibility consistent with the crystal-field scheme.

II. CALCULATED GROUND STATE ELECTRONIC STRUCTURE

The LDA calculation presented in this paper are performed with a full-potential (FP) linearized muffin-tin orbital (LMTO).[15] In the FP-LMTO method, the one-electron ground state is determined by solving a wave equation (in the present case scalar relativistic approximation to the Dirac equation) via a variational method. The one-electron wave function consists of a linear combination of linear muffin-tin orbital basis functions, with the expansion coefficients being determined from a variational procedure. In devising the ba-

sis functions for the valence electrons, the crystal is divided into muffin-tin sphere regions and an interstitial region. Inside the nonoverlapping muffin-tin spheres, the muffin-tin orbitals (MTO's) Φ are a product of spherical harmonics and a numerical solution of the radial wave equation (from a spherical muffin-tin potential) augmented by its energy derivative. Further the MTO is calculated at a suitable energy E_ν. In the interstitial region the basis function is a Bloch sum of Hankel or Neumann functions (which are analytical solutions of Helmholtz's equation). The two sets of basis functions are continuously and differentiably matched at the muffin-tin sphere. In the present calculations we used Pu $6p$, $7s$, $7p$, $5d$, and $6d$ and O $2s$, $2p$, and $3d$ basis functions. PuO_2 has the CaF_2 structure with a lattice constant $a = 5.2396$ Å. The k space was sampled using the special k-point method with 20 points in the irreducible part of the Brillouin zone.

The eigenfunctions for the core electrons are solutions to the single electron wave equation for a spherical average of the potential inside the muffin tin. The one-electron effective potential is determined using the local density approximation (LDA) to density functional theory,[16] in which the Coulomb potential is calculated from the Poisson equation, and the exchange-correlation potential has the von Barth-Hedin parametrization.[17] The potential at each iteration is determined utilizing the charge density determined from the eigenfunctions of the previous iteration. The true ground state energy as well as the eigenfunctions are obtained from a self-consistency procedure. The corresponding total crystal energy $E_{\rm tot}$ is

$$E_{\rm tot}[n(\mathbf{r})] = T_s[n(\mathbf{r})] + E_N[n(\mathbf{r})] + E_H[n(\mathbf{r})] + E_{\rm xc}[n(\mathbf{r})], \tag{1}$$

where the contributions are the kinetic energy $T_s[n(\mathbf{r})]$, the electron-nuclear interaction $E_N[n(\mathbf{r})]$, the Hartree electron-electron interaction energy $E_H[n(\mathbf{r})]$, and finally the exchange-correlation energy $E_{\rm xc}[n(\mathbf{r})]$; $n(\mathbf{r})$ being the charge density. The symmetry constrained calculations of the crystal-field splitting described in Sec. III need some correction to the former functional which we will be discussed also in Sec. III and in Appendix A.

The calculated valence electron structure is similar for all the actinide dioxides since one is obtained from the other by increasing the nuclear charge by one and adding a localized $5f$ electron. The lattice constant decreases by as little as 4% between ThO_2 and PuO_2, due to contraction arising from incomplete screening of the additional nuclear charge. The calculated valence bandwidth is about 5 eV (Fig. 1) and the calculate band gap between valence and conduction electron states is 4.6 eV for PuO_2 and marginally less for UO_2. The plutonium $6d$ and oxygen $2p$ states hybridize with the result that there are about 0.65 $6d$ electrons in the 12 (including spin degeneracy) oxygen-$2p$ derived valence bands with a corresponding reduction of the number of oxygen $2p$ electrons. The relatively small bandgap and large valence bandwidth compared with ionic compounds of the fluorite structure are the reason that the ionic model is not particularly appropriate for PuO_2 and the shape of the $6d$ charge density

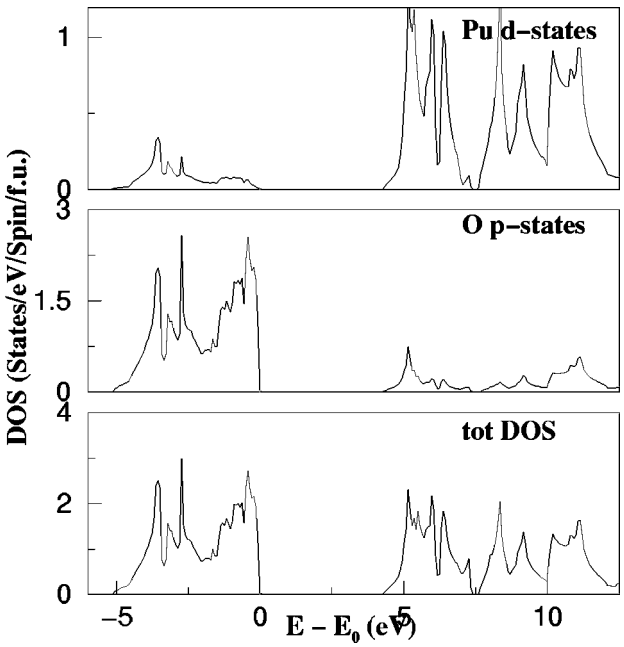

FIG. 1. Calculated partial density of states: Pu d states (upper panel) and O p states (middle panel), and total state density of PuO_2 (lower panel). E_0 indicates the energy of the highest occupied state.

contributes to the crystal field in addition to the lattice contribution. The size of the lattice contribution depends upon the amount of the charge transfer from Pu to O which is reduced below the ideal ionic value of 4 to about 3. The energy of the $5f$ states lies in the energy gap but since they are localized PuO_2 remains an insulator. The more general aspects of the electronic structure of PuO_2 in the present work are consistent with previous studies using spherically averaged charge densities.[19]

III. CONSTRAINED CALCULATIONS FOR THE 5*f*-STATES

The localized $5f$ states differ from both core and normal valence electron states. They are not true core states because the shell is open and the charge density is not spherical. They are not true valence electron states because, since they are localized, their occupation numbers are fixed, their hybridization with valence electron states is neglegible. The simplest approximation we can make for the $5f$ states is the Russell-Saunders coupling scheme which provides the standard model for the rare earths and restricts the $5f$ ground state to the maximum values of angular **L** and spin **S** momentum. Spin-orbit interaction is larger in actinides than in rare earths and in a more accurate theory an intermediate coupling scheme[18] would be used or, since the crystal fields are also strong, there might be some j mixing.[18] However, a ground state with $\mathbf{J}=\mathbf{L}+\mathbf{S}$ is relatively simple to handle in a first attempt and we adopt this approximation, leading to $S = 2$, $L = 6$, $J = 4$, and $g_J = 0.6$ for the f^4 configuration of PuO_2. The calculated value of $g_J = 0.643$ in intermediate coupling.

The Russell-Saunders $J = 4$ ground state is split by the

crystal-field originating from other conduction electrons into Γ_1, Γ_3, Γ_4, Γ_5 crystal field states and, in order to be able to find the energies of these states, we need to be able to reproduce their charge densities as accurately as possible. The first approximation that we make is to constrain the $5f$ occupation number to 4,

$$n_{5f}=n_{5f}^{+}+n_{5f}^{-}=4, \tag{2}$$

where the $\pm$ signs refer to spin up and down. Secondly, since the ground state of PuO_2 is nonmagnetic, the spin density is constained to be zero everywhere (as we shall see below, this constraint is consistent with our calculated Γ_1 ground state)

$$m_{5f}^{s}=n_{5f}^{+}-n_{5f}^{-}=0, \tag{3}$$

where m_{5f}^{s} is the spin component of the $5f$ magnetic moment. The radial $5f$ charge density is then

$$n_{5f}(r)=n_{5f}|\phi_{5f}^{+}(r)|^2+n_{5f}^{-}|\phi_{5f}^{-}(r)|^2 \tag{4}$$

and once the correct angular, aspherical part is calculated (as described below), the $5f$ density is added to the core and conduction electron densities to obtain the total density. Thus the radial functions are recalculated from the Pauli equation at each iteration and the distribution of radial $5f$ charge is a part of the variational calculation whereas the $5f$ occupation numbers are fixed as in a free atom calculation.

The aspherical part of the $5f$ charge density is determined by the crystal-field state and is therefore also constrained. As a first approximation we use the standard model for the rare earths to construct the charge density for each crystal-field state. Since the crystal-field states are mutually orthogonal linear combinations of the components $|J,M=-J,J\rangle$ of the four electron $2J+1$ degenerate ground state determined by symmetry, they may be decomposed into linear combinations of their single electron component states through the appropriate Clebsch-Gordon technology. Any crystal-field state may therefore be decomposed into linear combinations of single electron states which are products of spherical harmonics, occupation numbers and the above defined radial functions as shown in Appendix B. The total energy of the entire electron system may then be calculated for each crystal-field state with no shape restrictions placed upon the conduction electrons whose density is therefore allowed to shield the Coulomb and exchange fields of the $5f$ electrons. This approach goes beyond the conventional model which relies upon perturbation theory and conduction electron states which are independent of the crystal fields. Since each crystal-field state is the ground state of a given symmetry (there are no repeated irreducible representations for PuO_2) the variational nature of the Hohenberg-Kohn theorem implies that self-consistent calculations should yield the total energy of each crystal-field state correctly.[20,21] The crystal-field excitation energies are then calculated as differences between the total energies of crystal-field states.

A new aspect of the self-interaction problem emerges for this approach to crystal-field calculations. The total energies of two different aspherical f CEF charge densities in a free atom differ in a density functional LDA calculation. This is an unphysical crystal-field splitting: in a free atom the charge density is always aspherical if there are open shells but the density is free to rotate in an isotropic environment. The rotational degree of freedom is removed in a density functional LDA calculation, reducing the degeneracy of the ground state. The internal aspherical interactions of the $5f$ states are already included by the construction of **J** and the density functional must be modified to exclude any symmetry breaking due to interactions between the aspherical $5f$ density at a given site. We therefore subtract the interaction of the nonspherical part of the $5f$-electron density with itself from the total energy functional and remove its contribution to the Hartree and exchange-correlation potentials for the $5f$ electrons. The energy functional in Eq. (1), disregarding nuclei contributions, becomes (see Appendix A)

$$\begin{aligned} E=\sum_i n_i\epsilon_i-\frac{1}{2}\int\frac{\overline{n}(\mathbf{r})\overline{n}(\mathbf{r}')d\mathbf{r}d\mathbf{r}'}{|\mathbf{r}-\mathbf{r}'|}-\int\frac{\overline{n}(\mathbf{r})n_{5f}^{ns}(\mathbf{r}')d\mathbf{r}d\mathbf{r}'}{|\mathbf{r}-\mathbf{r}'|} \\ +\int\{\epsilon_{\mathrm{xc}}[\overline{n}]-\mu_{\mathrm{xc}}[\overline{n}]\}\overline{n}(\mathbf{r})d\mathbf{r} \\ -\int n_{5f}^{ns}(\mathbf{r})\frac{\delta\mu_{\mathrm{xc}}[\overline{n}]}{\overline{n}}\overline{n}(\mathbf{r})d\mathbf{r}, \end{aligned} \tag{5}$$

where n_i is the occupation number and ϵ_i is the Kohn-Sham eigenvalue of the ith level, $n_{5f}^{ns}(\mathbf{r})$ is the nonspherical part of the $5f$ electron charge density, $\overline{n}(\mathbf{r})$ is the difference between the total density and the nonspherical part of the $5f$ electrons, $\overline{n}(\mathbf{r})\equiv n(\mathbf{r})-n_{5f}^{ns}(\mathbf{r})$, μ_{xc} is the exchange correlation potential, $\mu_{\mathrm{xc}}\equiv\delta E_{\mathrm{xc}}/\delta n$, and ϵ_{xc} is coming from the LDA, $E_{\mathrm{xc}}\simeq\int n(\mathbf{r})\epsilon_{\mathrm{xc}}(n)d\mathbf{r}$.

The crystal-field energies are then degenerate in a spherical conduction electron density and the crystal-field splitting entirely due to the crystalline environment, as in the perturbation theoretic approach. The method we use to calculate crystal-field splittings is essentially independent on the particular constraints chosen for the radial part of the f density. Self-interaction corrected LDA or LDA with a constraining step potential (for the core electrons) outside the MT radius produced no significative difference compared to usual LDA.[14] This can be attributed to two main reasons. First, we are not calculating crystal field parameters from potential integrals but are dealing with total energies which are variationally more stable to small differences in charge densities. Secondly, the crystal field affects only the nonspherical part of the f density. Changing constraints on the radial part tends to change all the calculated crystal-field levels by the same amount and does not affect the energy differencies.

IV. RESULTS AND ANALYSIS

The calculated crystal-field excitation energies are shown in Table I. We obtain a singlet Γ_1 ground state and the first excited state is Γ_4 with an excitation energy of 99 meV in resonable agreement with the inelastic neutron scattering measurement of 123 meV.[2]

It is a simple matter to calculate the bare magnetic susceptibility as a function of temperature for PuO_2 and, to il-

TABLE I. Calculated and esperimental CF levels for PuO_2. Values are given with respect to the calculated ground state Γ_1. Measured values for $\Gamma_1 \rightarrow \Gamma_3$ and $\Gamma_1 \rightarrow \Gamma_5$ transitions are absent because their matrix elements are zero.

PuO_2	Calc. (meV)	Exp.[2] (meV)	Exp.[1] (meV)
Γ_1	0	0	0
Γ_4	99	123	284
Γ_3	162		
Γ_5	208		

lustrate the problem, we have done so in several approximations (Fig. 2). First, for a single $\Gamma_1 \rightarrow \Gamma_4$ transition with an energy of 284 meV the van Vleck temperature independent susceptibility measured by Raphael and Lallement[1] is reproduced at low temperatures but at higher temperatures the susceptibility decreases due to excited state occupation. For the measured $\Gamma_1 \rightarrow \Gamma_4$ transition with an energy of 123 meV

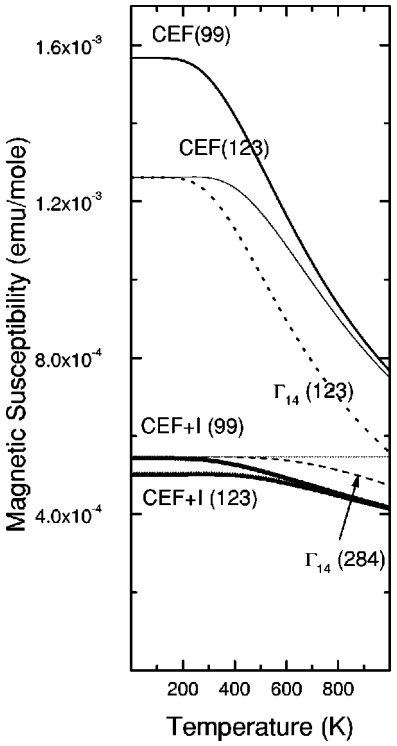

FIG. 2. The magnetic susceptiblity of PuO_2. The measurements are the temperature independent straight dotted line and the calculated bare susceptibility with a sole $\Gamma_1 \rightarrow \Gamma_4$ excitation energy of 284 meV which fits the data at $T=0$ is the dashed line labeled $\Gamma_{14}(284)$. The corresponding calculated bare susceptibility with a sole $\Gamma_1 \rightarrow \Gamma_4$ excitation energy of 123 meV which fits the neutron-scattering data is the dotted line labeled Γ_{14} (123). Adding calculated additional crystal-field transitions to the 123 meV transition produces the improvement shown by the solid line labeled CEF(123) whereas replacing the measured $\Gamma_1 \rightarrow \Gamma_4$ excitation energy by the calculated 99 meV transition produces the solid line labeled CEF(99). The effect of using the antiferromagnetic molecular field deduced from that of UO_2 to enhance the latter two bare susceptibilities results in the full curves labeled CEF+I.

the susceptibility is both too large and decreases above 300 K due to population of the excited state. Secondly, we added the calculated Γ_3 and Γ_5 crystal-field levels: (a) replacing the calculated $\Gamma_1 \rightarrow \Gamma_4$ of 99 meV by the measured 123 meV and (b) using the calculated levels with $\Gamma_1 \rightarrow \Gamma_4 = 99$ meV. The susceptibility obtained from the calculated crystal-field levels is also far too large and decreases above 200 K. Our conclusion is that it is not possible, for a $J=4$ ground state, to reproduce neither the magnitude of the measured susceptibility with a $\Gamma_1 \rightarrow \Gamma_4$ exitation energy of less than 280 meV nor the temperature dependence, since excited state population always leads to a significant decrease in the susceptibility at a temperature (in K) which is about three times the first excitation energy (in meV).

Detailed investigation of the inconsistency between the neutron scattering results and susceptibility measurements has been made by Santini and his collaborators.[23] Of the possible mechanisms able to resolve the anomaly, they consider antiferromagnetic exchange to be the most likely. We may estimate the magnitude of antiferromagnetic exchange in PuO_2 in the following way. The susceptibility of antiferromagnetic UO_2 has been measured by Nasu[26] who found a Curie-Weiss law with $\chi = 1.28/(T-\theta_p)$ emu/mole, corresponding to a paramagnetic Neel temperature $\theta_p = -220$ K with an effective moment of $3.2\mu_B$. Since

$$1/\chi = 1/\chi_0 - \lambda, \tag{6}$$

the exchange (or molecular) field which enhances the susceptibility is $\lambda = -220/1.28$ mole/emu for UO_2. In both LSDA and model Hamiltonians the isotropic part of the exchange interaction is between the spin components of the moment[27] and a Heisenberg model Hamiltonian

$$H = -\frac{1}{2}\sum_{ij} J_{ij}\mathbf{S_i}\cdot\mathbf{S_j} \tag{7}$$

produces the molecular field

$$\lambda = \left[\frac{(g_J-1)}{g_J\mu_B}\right]^2 \langle m_z\rangle \sum_j J_{ij} \tag{8}$$

acting on the total moment m_z per atom. The value of λ deduced from the magnetic susceptibility for UO_2 corresponds to an exchange interaction coupling constant $J = 7.3$ meV for nearest-neighbor interactions and 12 nearest neighbors with $g_J(UO_2) = 4/5$ for the f^2 Russell-Saunders ground state. The calculated value of g_J for UO_2 is 0.821 in intermediate coupling therefore 0.8 is a good approximation.

The mechanism for antiferromagnetism that occurs naturally from the electronic structure calculations is that the $5f$ moment polarizes the valence electrons locally at the actinide sites and that the polarization is transmitted between sites by the $6d$ admixture in the valence bands. The strength of the exchange interactions will depend upon the amount of induced $6d$ moment which in turn depends upon the amount of $6d$ admixture in the valence bands. Since our calculated valence electronic structures of UO_2 and PuO_2 are almost identical, the valence conduction electron gap being slightly larger in PuO_2, we argue that to a good first approximation,

the exchange interactions J in UO_2 and PuO_2 are about the same. However, the g factor of PuO_2 is $g_J(PuO_2)=3/5$ and the molecular field is 7.1 times larger than in UO_2 due to the g factor scaling in Eq. (8). With this value of the molecular field we have recalculated χ according to Eq. (6) and plotted the results in Fig. 2 for the two cases where the $\Gamma_1 \rightarrow \Gamma_4$ excitation energy is 99 and 123 meV. The evaluation of the molecular field of PuO_2 through the molecular field of UO_2 leaves no free parameters and we believe that the major part of the anomaly between the two experiments is resolved. We are not, however, able to remove the temperature dependence of the susceptibility above 300 K and, given the energy scales involved, do not believe it can be done. More recent, unpublished, susceptibility measurements by Kolberg[28] up to 300 K confirm the original measurements of Raphael and Lallement[1] but were not extended to higher temperatures.

V. CONCLUSIONS

The calculated $\Gamma_1 \rightarrow \Gamma_4$ excitation energy of 99 meV is consistent with the inelastic-neutron-scattering result[2] of 123 meV. We also present the other crystal-field excitation energies which belong to the lowest J multiplet. The computational method we have used is based upon total energy diffences. Each crystal-field energy has been calculated by constraining the angular part of the plutonium $5f$-electron density, the radial part being calculated self-consistently. Since the crystal symmetry and lattice constant are identical for all the calculated levels the radial part of the $5f$-electron density is also essentially unchanged. There should therefore be some cancellation of errors occuring in LDA.

The similarity of the calculated valence charge densities in UO_2 and PuO_2 may also be used to argue that there is a simple scaling of the crystal-field parameters in the spin Hamiltonian[24]

$$H = V_4\beta[\hat{O}_4^0 + 5\hat{O}_4^4] + V_6\gamma[\hat{O}_6^0 - 21\hat{O}_6^4], \tag{9}$$

where β and γ are Stevens factors,[22] as has been done for NpO_2.[25] Since UO_2 and PuO_2 both have $J=4$ ground states (but with different parentage) the operator equivalents $\hat{O}_m^n$ are the same but the Stevens factors differ. The crystal-field parameters V_m are proportional to radial integrals r^n which have been evaluated for actinide $4+$ ions. Due to contraction of the wave functions r^n is reduced by about 25% for $n=4$ and 35% for $n=5$ from UO_2 to PuO_2 and there is a large change in β which is responsible for a change of ground state from Γ_5 to Γ_1. Santini[23] has shown that the $\Gamma_1 \rightarrow \Gamma_3$ excitation energy scales to about 160 meV which is close to the calculated excitation energy. Similarly, a reasonable scaling of the measured molecular field in UO_2 leads to antiferromagnetic exchange enhancement in PuO_2 which lowers the calculated magnetic susceptibility and produces agreement with measurements at low temperatures. We are not, however, able to explain the anomalous lack of temperature dependence of the magnetic susceptibility at high temperature. The most obvious refinements of the present work would be to use intermediate coupling, remove the restriction to the lowest J multiplet and to consider the dynamic Jahn-Teller effect.[23]

ACKNOWLEDGMENTS

The authors are grateful to G.H. Lander for bringing the anomaly in the experiments to our attention and to D. Kolberg for many discussions. M.C.T., L.N., and O.E. are grateful to The Swedish Natural Science Foundation (VR) and the Swedish Foundation for Strategic Research (SSF) for supporting this work. M.C.T. acknowledges the European Commission for support given in the frame of the program ''Human Capital and Mobility.''

APPENDIX A: THE CEF LDA ENERGY FUNCTIONAL

In the expression for the total energy Eq. (1) one needs to correct the Hartree part and the exchange correlation part. If the total density is $n(\mathbf{r})=\overline{n}(\mathbf{r})+n_f^{\rm ns}(\mathbf{r})$, where $n(\mathbf{r})$ is the nonspherical f charge density then the Hartree energy should be

$$E_H[n] = \frac{1}{2}\int \frac{\overline{n}(\mathbf{r})\overline{n}(\mathbf{r}')d\mathbf{r}d\mathbf{r}'}{|\mathbf{r}-\mathbf{r}'|} + \int \frac{\overline{n}(\mathbf{r})n_f^{\rm ns}(\mathbf{r}')d\mathbf{r}d\mathbf{r}'}{|\mathbf{r}-\mathbf{r}'|}, \tag{A1}$$

where a third term in $n_f^{\rm ns}(\mathbf{r})n_f^{\rm ns}(\mathbf{r}')$ is explicitly excluded.

The exchange and correlation energy

$$E_{\rm xc}[n] = \int n(\mathbf{r})\epsilon_{\rm xc}(n)d\mathbf{r} = \int \{\overline{n}(\mathbf{r})+n_f^{\rm ns}(\mathbf{r})\}\epsilon_{\rm xc}[\overline{n}+n_f^{\rm ns}]d\mathbf{r} \tag{A2}$$

also contains $n_f^{\rm ns}(\mathbf{r})$ interactions which must be excluded. Since the nonspherical f density is relatively small

$$E_{\rm xc}[n] = \int \{\overline{n}(\mathbf{r})+n_f^{\rm ns}(\mathbf{r})\}\left\{ \epsilon_{\rm xc}[\overline{n}] + n_f^{\rm ns}(\mathbf{r})\frac{\delta\epsilon_{\rm xc}[n]}{\delta n}\bigg|_{n=\overline{n}}\right\}d\mathbf{r} \tag{A3}$$

the term in $n_f^{\rm ns}(\mathbf{r})n_f^{\rm ns}(\mathbf{r})$ should be dropped, therefore,

$$E_{\rm xc}[n] = \int \overline{n}(\mathbf{r})\epsilon_{\rm xc}[\overline{n}]d\mathbf{r} + \int n_f^{\rm ns}(\mathbf{r})\left\{ \epsilon_{\rm xc}[\overline{n}] + \overline{n}(\mathbf{r})\frac{\delta\epsilon_{\rm xc}[n]}{\delta n}\bigg|_{n=\overline{n}}\right\}d\mathbf{r} \tag{A4}$$

or

$$E_{\rm xc}[n] = \int \overline{n}(\mathbf{r})\epsilon_{\rm xc}[\overline{n}]d\mathbf{r} + \int n_f^{\rm ns}(\mathbf{r})\mu_{\rm xc}[\overline{n}]d\mathbf{r}. \tag{A5}$$

Now the wave equation

$$\left(-\frac{1}{2}\nabla^2 + V_N + V_H + \mu_{\rm xc}\right)\psi_i = \epsilon_i\psi_i \tag{A6}$$

should be modified, with the first two terms remaining unchanged and

$$V_H = \int \frac{\{\overline{n}(\mathbf{r}) + n_f^{\rm ns}(\mathbf{r})\} d\,\mathbf{r}}{|\mathbf{r}-\mathbf{r}'|} \tag{A7}$$

for non-f states, and

$$V_H^f = \int \frac{\overline{n}(\mathbf{r}) d\,\mathbf{r}}{|\mathbf{r}-\mathbf{r}'|} \tag{A8}$$

for f states. The exchange correlation potential should also be modified

$$\mu_{\rm xc}[n] = \mu_{\rm xc}[\overline{n}] + n_f^{\rm ns}(\mathbf{r}) \frac{\delta \mu_{\rm xc}[\overline{n}]}{\delta \overline{n}} \tag{A9}$$

for non-f states and

$$\mu_{\rm xc}^f[n] = \mu_{\rm xc}[\overline{n}] \tag{A10}$$

for f states.

Now the kinetic energy becomes

$$\begin{aligned} T_s[n] = \sum_i n_i \epsilon_i - \int V_N(\mathbf{r}) n(\mathbf{r}) d\mathbf{r} - \int V_H(\mathbf{r}) \overline{n}(\mathbf{r}) d\mathbf{r} \\ - \int V_H^f(\mathbf{r}) n_f^{\rm ns}(\mathbf{r}) d\mathbf{r} - \int \left\{ \mu_{\rm xc}[\overline{n}] \right. \\ \left. + n_f^{\rm ns}(\mathbf{r}) \frac{\delta \mu_{\rm xc}[\overline{n}]}{\delta \overline{n}} \right\} \overline{n}(\mathbf{r}) d\mathbf{r} - \int \mu_{\rm xc}[\overline{n}] n_f^{\rm ns}(\mathbf{r}) d\mathbf{r} \end{aligned} \tag{A11}$$

which susbstituted in Eq. (1), yields Eq. (5).

APPENDIX B: THE CEF CHARGE DENSITY

A crystal-field state can be written as a linear combination of $|J,M_J\rangle$ states (since they span the subspace of the lowest J multiplet):

$$\Psi_i^{\rm CEF} = \sum_{M_J} C_{M_J} |J, M_J\rangle. \tag{B1}$$

In order to construct the density it is necessary to change to a single electron basis $|ll, \ldots, lm_{l_1} m_{l_2}, \ldots, m_{l_N}\rangle$. For notational simplicity we restrict to two electrons since the extension to another value of N is trivial. First,

$$\begin{aligned} |LSJM_J\rangle &= \sum_{M_L, M_S} \begin{pmatrix} L & S & J \\ M_L & -M_S & -M_J \end{pmatrix} \\ &\quad \times \sqrt{2J+1} (-1)^{L-S+M_J} |LSM_S M_L\rangle \end{aligned} \tag{B2}$$

$$= \sum_{M_L, M_S} C_{M_S, M_L} |LSM_S M_L\rangle \tag{B3}$$

and

$$|LSM_S M_L\rangle = |llLM_L\rangle |ssSM_S\rangle, \tag{B4}$$

where

$$\begin{aligned} |llLM_L\rangle &= \sum_{m_{l_1}, m_{l_2}} \begin{pmatrix} l & l & L \\ m_{l_1} & m_{l_2} & -M_L \end{pmatrix} \\ &\quad \times \sqrt{2L+1} (-1)^{M_L} |llm_{l_1} m_{l_2}\rangle, \end{aligned} \tag{B5}$$

$$\begin{aligned} |ssSM_S\rangle &= \sum_{m_{s_1}, m_{s_2}} \begin{pmatrix} s & s & S \\ m_{s_1} & m_{s_2} & -M_S \end{pmatrix} \\ &\quad \times \sqrt{2S+1} (-1)^{M_S} |ssm_{s_1} m_{s_2}\rangle. \end{aligned} \tag{B6}$$

Hence the entire expansion

$$\begin{aligned} \Psi_i^{\rm CEF} = \sum_{m_{l_1}, m_{l_2}} \sum_{m_{s_1}, m_{s_2}} C(m_{l_1}, m_{l_2}, m_{s_1}, m_{s_2}) |llm_{l_1} m_{l_2}\rangle \\ \times |ssm_{s_1} m_{s_2}\rangle, \end{aligned} \tag{B7}$$

where the coefficients $C(m_{l_1}, m_{l_2}, m_{s_1}, m_{s_2})$ are easily deducible by comparing all the previous equations with Eq. (B7). The single electron density is then obtained integrating

$$n_i^{\rm CEF}(\underline{r}_1) = 2 \int d\underline{r}_2 [\Psi_i^{\rm CEF}(\underline{r}_1, \underline{r}_2)]^* \Psi_i^{\rm CEF}(\underline{r}_1, \underline{r}_2). \tag{B8}$$

[1] G. Raphael and R. Lallement, Solid State Commun. **6**, 383 (1968).

[2] S. Kern, R.A. Robinson, H. Nakotte, G.H. Lander, B. Cort, P. Watson, and F.A. Vigil, Phys. Rev. B **59**, 104 (1999).

[3] K. Hummler and M. Fähnle, Phys. Rev. B **53**, 3272 (1996); **53**, 3290 (1996); P. Uebele, K. Hummler, and M. Fähnle, *ibid.* **53**, 3296 (1996).

[4] L. Steinbeck, M. Richter, U. Nitzsche, and H. Eschrig, Phys. Rev. B **53**, 7111 (1996).

[5] L. Steinbeck, M. Richter, H. Eschrig, and U. Nitzsche, Phys. Rev. B **49**, 16 289 (1994).

[6] M. Richter, P.M. Oppeneer, H. Eschrig, and B. Johansson, Phys. Rev. B **46**, 13 919 (1992).

[7] M. Divis, M. Richter, H. Eschrig, and L. Steinbeck, Phys. Rev. B **53**, 9658 (1996).

[8] G.H.O. Daalderop, P.J. Kelly, and M.F.H. Schuurmans, Phys. Rev. B **53**, 14 415 (1996).

[9] P. Blaha, K.H. Schwartz, and P.H. Dederichs, Phys. Rev. B **37**, 2792 (1988).

[10] R. Coehoorn, K.H.J. Buschow, M.W. Dirken, and R.C. Thiel, Phys. Rev. B **42**, 4645 (1990)

[11] J.P. Perdew and A. Zunger, Phys. Rev. B **23**, 5048 (1981).

[12] A. Svane and O. Gunnarsson, Europhys. Lett. **7**, 171 (1988); S.V. Beiden, W.M. Temmerman, Z. Szotek, and G.A. Gehring, Phys. Rev. Lett. **79**, 3970 (1997).

[13] M.S.S. Brooks, O. Eriksson, J.M. Wills, and B. Johansson, Phys. Rev. Lett. **79**, 2546 (1997).

[14] M. Colarieti Tosti, O. Eriksson, L. Nordström, M. S. S. Brooks,

and J. M. Wills, J. Magn. Magn. Mater. (to be published).
[15] J. M. Wills, O. Eriksson, M. Alouani, and D. L. Price, in *Electronic Structure and Physical Properties of Solids*, edited by H. Dressey (Springer Verlag, Berlin, 2000), p. 148.
[16] P. Hohenberg and W. Kohn, Phys. Rev. **136**, B864 (1964); W. Kohn and L.J. Sham, *ibid.* **140**, A1133 (1965).
[17] U. von Barth and L. Hedin, J. Phys. C **5**, 1629 (1972).
[18] S.-K. Chan and D. J. Lam, in *The Actinides: Electronic Structure and Related Properties*, edited by A. J. Freeman and J. B. Darby, Jr. (Academic Press, New York, 1974), p. 1.
[19] P.J. Kelly and M.S.S. Brooks, J. Chem. Soc., Faraday Trans. 2 **83**, 1189 (1987).
[20] O. Gunnarsson and B.I. Lundqvist, Phys. Rev. B **13**, 4274 (1976).
[21] U. von Barth, Phys. Rev. A **20**, 1693 (1979).
[22] J. Jensen and A. R. Mackintosh, *Rare Earth Magnetism* (Oxford University Press, Oxford, 1991).
[23] P. Santini and L. Sieffert (unpublished).
[24] G. Amoretti, A. Blaise, R. Caciuffo, J.M. Fournier, M.T. Hutchings, R. Osborn, and A.D. Taylor, Phys. Rev. B **40**, 1856 (1989)
[25] G. Amoretti, A. Blaise, R. Caciuffo, D. Di Cola, J.M. Fournier, M.T. Hutchings, G.H. Lander, R. Osborn, A. Severing, and A.D. Taylor, J. Phys.: Condens. Matter **4**, 3459 (1992).
[26] S. Nasu, Jpn. J. Appl. Phys. **5**, 1001 (1966).
[27] M.S.S. Brooks, T. Gasche, S. Auluck, L. Nordström, L. Severin, J. Trygg, and B. Johansson, J. Appl. Phys. **70**, 5972 (1991).
[28] D. Kolberg, Ph.D. thesis, TU-Braunschweig, 2001.